J Solid State Electrochem (2006) 11: 59–64
DOI 10.1007/s10008-005-0067-x

ORIGINAL PAPER

Songli Li · Shaorong Wang · Huaiwen Nie
Ting-lian Wen

A direct-methane solid oxide fuel cell with a double-layer anode

Received: 5 July 2005 / Revised: 15 August 2005 / Accepted: 20 August 2005 / Published online: 24 September 2005

Abstract A tubular anode-supported solid oxide fuel cell with a double-layer anode for the direct conversion of CH_4 has been prepared and operated at 800 °C successfully. The double-layer anode was composed of NiO–YSZ and CoO–NiO–SDC acting as supporting layer and active reforming layer, respectively. At 800 °C, a maximum power density of 350 mW cm^{-2} was obtained with CH_4 as fuel and air as oxidant. The time-dependent impedance spectra of the tubular cell were examined and discussed. No carbon deposition was observed on the surface of the anode when the cell was operated at a constant current density of 250 mA cm^{-2}.

Keywords Double-layer anode · SOFC · CH_4 fuel · Carbon deposition

Introduction

Solid oxide fuel cell (SOFC) has the potential of direct-using hydrocarbons as fuels [1]. Direct conversion means conversion in the SOFC without pre-mixing the fuel gas with steam or CO_2, and without processing the fuel before it enters the cell stack [2]. Carbon deposition at the nickel–YSZ cermet anode is the major obstacle in case of direct-using hydrocarbons, e.g. methane, as fuel [3]. A lot of research work has been done to overcome this problem. Perovskite oxides have been studied as new anode materials for methane fuel free of carbon deposition [4–8]. However, because of either low electrical conductivity or low electrochemical activity, the performance of the perovskite oxide as anode material of SOFC was very poor. Copper [9], as good electrical conductor, was reported to inhibit CH_4 pyrolysis. However, Cu is not as good an electrocatalyst as Ni. Furthermore, Cu has a relatively low melting point, and is thus not compatible with many high-temperature SOFC fabrication techniques. Besides nickel and copper, cobalt also exhibits a high electrical conductivity and electrochemical activity. Moreover, it was reported recently that cobalt could reduce carbon deposition during oxidative conversion of methane to syngas [10]. However, the high cost of cobalt may limit its extensive application when anode-supported cell is fabricated. Rare earth-doped ceria is known as a mixed ionic and electronic conductor under reducing atmospheres [11, 12], and has been used as anode material for the direct oxidation of methane [13], but the volume expansion during reduction may be a problem.

It is well known that mass transport through the anode produces substantial partial pressure gradients [14]. Thus, when methane is taken as fuel, the methane partial pressure decreases from the fuel gas stream to the anode surface to the anode/electrolyte interface, and the tendency to cause carbon deposition follow the reverse trend.

Considering both the cost and the performance aspects, a double-layer anode has been suggested in the present work for a tubular SOFC. The layer directly attached to the electrolyte consists of NiO–YSZ [(YSZ, 8 mol% Y_2O_3-doped ZrO_2); NiO:YSZ = 65:35 (weight ratio)] which is about 1 mm thick, is called the supporting layer. The layer exposed to the fuel gas consists of CoO–NiO–SDC (SDC, $Ce_{0.8}Sm_{0.2}O_2$; CoO:NiO:SDC = 13:52:35), which is active for partial oxidation of methane, called active reforming layer. A tubular type single cell is adopted because it has the benefit of easiness in sealing and large effective area. In order to supply sufficient oxygen ions for methane conversion [15, 16], the tubular cell was operated at a fairly large current density of 250 mA cm^{-2}. At the interface of Ni–YSZ/YSZ, CH_4 might first be partially oxidized into H_2 and CO and then further be oxidized into H_2O and CO_2. In the anode substrate, CH_4 might be reformed either by H_2O or CO_2. Although the tendency to cause carbon deposition increased in the anode away from the elec-

S. Li (✉) · S. Wang · H. Nie · T. Wen
Shanghai Institute of Ceramics, Chinese Academy of Science,
1295 Dingxi Road, 200050 Shanghai, P. R. China
E-mail: lisongli@mail.sic.ac.cn
Tel.: +86-21-52412057
Fax: +86-21-52413903

Table 1 Chemical compositions of the dipping slurries for 100 g ceramic powders (/g)

	TEA	Alcohol	Butanone	DOP	PEG	PVB
Anode	2.5–2.8	30	60	5.5–6	5.5–6	9.5–10
Electrolyte	2.5–2.8	140	140	4.5–5	4.5–5	3.5–3.8
Interlayer	3–3.2	120	150	2.2–2.5	2.2–2.5	5.5–5.8
Cathode	3.5–3.8	100	150	2.2–2.5	2.2–2.5	5.5–5.8

trolyte, the high catalytic activity of Co–Ni–SDC for methane reforming might further inhibit methane pyrolysis at the active reforming layer. As a result, no obvious carbon deposition was observed and CH_4 was directly conversed in the double-layer anode.

Experiments

Fabrication of the tubular SOFC

The tubular SOFC was fabricated by a consecutive dipping method. Before dipping, the slurries of all the components were prepared by a two-step ball-milling method. For example, the original oxide powders of the

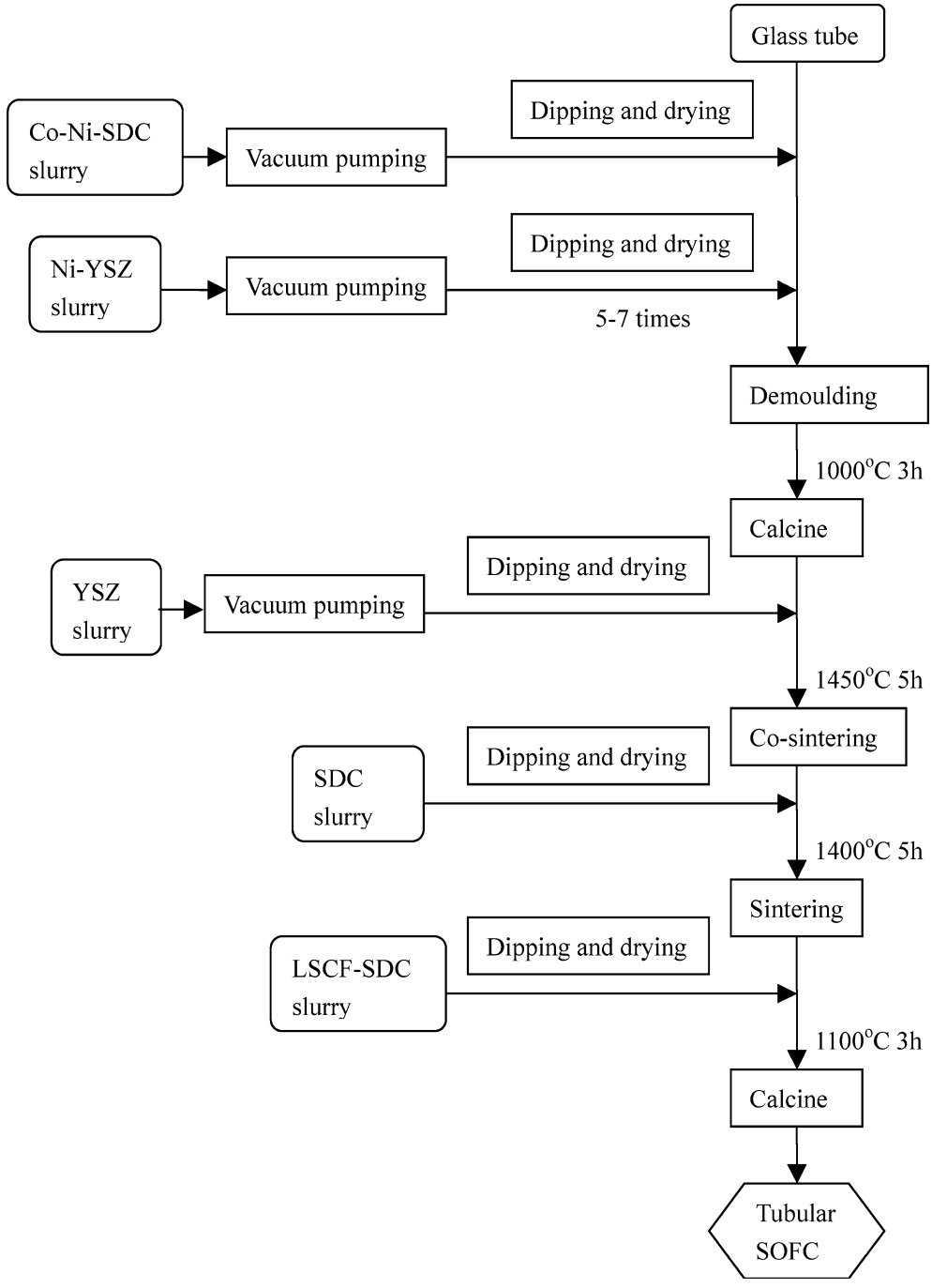

Fig. 1 Technological scheme of the preparation of the tubular solid oxide fuel cell (SOFC)

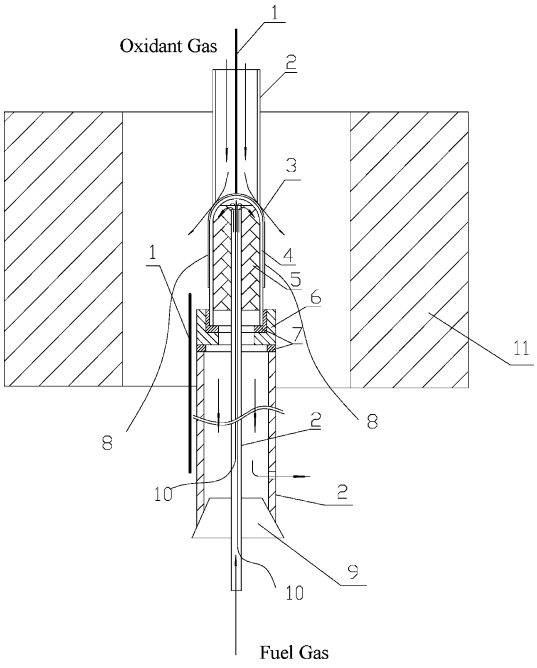

Fig. 2 Schematic drawing of the tubular SOFC setup: *1* thermocouples, *2* alumina tube, *3* Pt mesh, *4* SOFC, *5* nickel felt, *6* alumina substrate, *7* glass sealant, *8* Pt wire, *9* rubber bung, *10* Au wire, *11* furnace

anode (either NiO–YSZ or CoO–NiO–SDC) were first ball-milled with triethanolamine (TEA) in appropriate ratios in a mixture of alcohol and butanone solvents. Then, dibutyl *o*-phthalate (DOP), polyethylene glycol (PEG) and polyvinyl butyral (PVB) were added and ball-milled again till uniform slurry was formed. In the same way, the slurries of the YSZ electrolyte, the LSCF ($La_{0.6}Sr_{0.4}Co_{0.2}Fe_{0.8}O_3$)–SDC (LSCF:SDC = 70:30) cathode, and the SDC interlayer were prepared, separately. The exact amounts of the organic additives in the slurries are listed in Table 1.

The dipping process was carried out on a one-end-closed glass tube with an outside diameter of 10 mm. A complete technological scheme of the cell preparation was listed in Fig. 1. First, the anode active reforming layer was dipped once and then the anode supporting layer was dipped 5–7 times to reach a thickness of about 1 mm. After drying, the green anode tube was rolled out from the glass tube and calcined at 1,000 °C for 3 h. Then electrolyte was dipped on the surface of the green anode and co-sintered at 1,450 °C for 5 h. Finally, the SDC interlayer and cathode layer were dipped. The sintering temperature of the SDC interlayer and the cathode layer was 1,400 °C (5 h) and 1,100 °C (3 h) respectively. The effective working area of the dipped tubular SOFC was 8∼10 cm^2 according to the cathode area.

Measurements of cell performance

The output performance of the tubular SOFC was tested under the control of a constant voltage power supply and a variable resistor. The current and voltage were

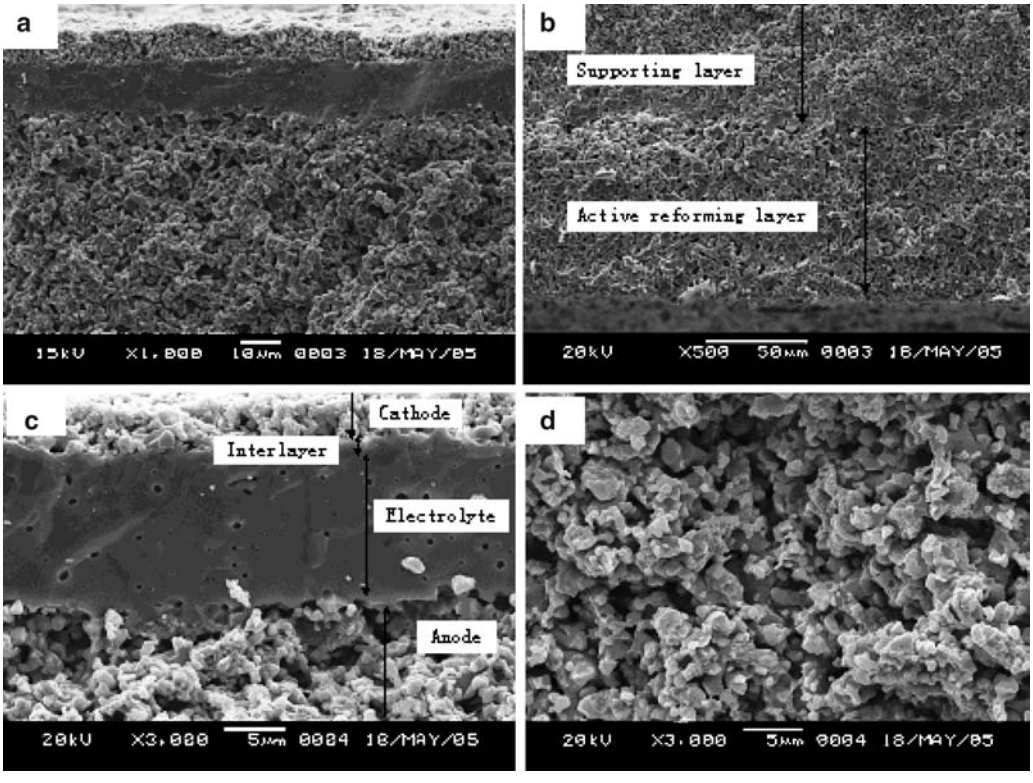

Fig. 3 Cross-section SEM images of the tubular SOFC: **a** sandwich structure before reduction, **b** double-layer anode before reduction, **c** sandwich structure after cell test, **d** supporting layer close to the electrolyte after cell test

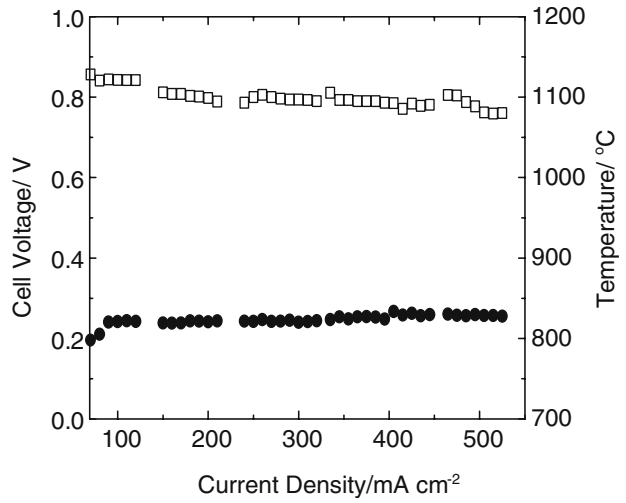

Fig. 4 Time-dependent characteristics of the tubular cell with $H_2$and CH_4 fuel at a constant current density of 250 mA cm^{-2}; *open square* cell voltage, *filled circle* temperature

measured by ampere meter (0.1 mA) and voltmeter (0.01 mV) in high precision. EIS measurements were carried out at open-circuit condition on Model IM6e electrochemical workstation (Zahner, GmbH, Germany) with an AC signal of 20 mV amplitude. Measurements were carried out in the frequency range of $1\sim10^5$ Hz.

As shown in Fig. 2, the fabricated tubular single cell was installed into an alumina tube with two glass rings as sealant. Nickel felt and Au wires were used as current collector for the anode, and Pt mesh and Pt wires were used for the cathode. Two thermocouples were used to control the SOFC temperature. The temperature at the top of the SOFC was regarded as the SOFC temperature. In the first stage of the cell operation, the cell was heated to 850 °C at a rate of 5 °C min^{-1}. After the cell was sealed gastight, the cell temperature was slowly decreased to 800 °C. The anode was reduced in hydrogen for 1 h and then switched to CH_4 for cell performance measurements. A current density of 250 mA cm^{-2} was maintained during operation, except for the I–V characteristics and EIS measurements. CH_4 was fed with a flow rate of 50 ml min^{-1} and air, as oxidant gas in the cathode, was fed with a flow rate of 200 ml min^{-1}.

The morphology of the cell was studied by scanning electron microscopy (SEM; S570, HITACHI, Japan) before and after the cell operation.

Results and discussion

Microstructures of the tubular SOFC

Figure 3a and b shows the cross-section SEM images of the tubular SOFC before reduction. As seen in Fig. 3a, both porous electrodes and the dense electrolyte have been obtained homogeneously. The anode substrate was thick and gave a support for the whole cell, while the electrolyte was a thin film (about 15 μm) so the ohmic resistance was decreased. In Fig. 3b, the active reforming layer, about 70 μm thick, was in close contact with the supporting layer. Both layers have uniform structure and no obvious segregation between the double layers was observed at the interface.

Figure 3c and d shows microstructures of the tubular SOFC after the cell test. As shown in Fig. 3c, both the anode and the cathode had porous and homogeneous microstructures and tightly bonded to the electrolyte. The electrolyte was a dense film with only small pin holes of about 1 μm observed in its body. The dense electrolyte can prevent gas diffusion from the anode to the cathode and vice versa. Due to the similar microstructure of the SDC interlayer and the YSZ electrolyte, it is hard to distinguish them directly in Fig. 3c. When it was analyzed by the backscattered-electron image at the same place in Fig. 3c (not shown here), the thickness of the dense SDC interlayer is only about 1∼2 μm. However, the thin SDC interlayer is sufficient to prevent the reaction between the LSCF–SDC cathode and the YSZ electrolyte [17, 18]. Figure 3d shows the morphology of the supporting anode close to the electrolyte film. The pores and particles are uniformly distributed in the anode. The grain boundaries of the particles are clear and most of the particles are 1–2 μm in diameter. No obvious sintering of the anode is observed.

Output performance of the cell

Figure 4 shows the time-dependent operating temperature and cell voltage at a constant current density of 250 mA cm^{-2}. Data measured at other than 250 mA cm^{-2} was eliminated from this plot and discussed in the following. As seen in Fig. 4, the cell voltage decreased slowly from 0.85 to 0.76 V in

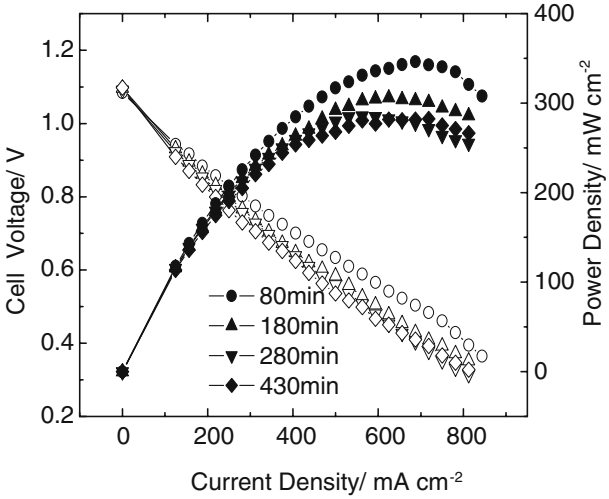

Fig. 5 Time-dependent change of output performances of the tubular SOFC with CH_4 fuel at 800 °C, in which *open symbols* refer to cell voltage, *closed symbols* refer to power density

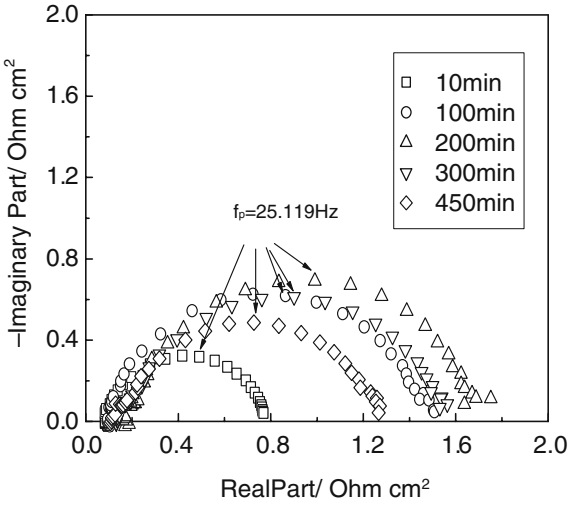

Fig. 6 Plot of time-dependent AC impedance spectra of the tubular SOFC in the frequency range of $1\sim10^5$ Hz with CH_4 fuel at 800 °C

450 min and the operating temperature of the tubular SOFC increased in a slow and steady rate. It is well known that the partial oxidation of CH_4 and further oxidation of CO and H_2 are exothermic, while the following reforming reactions (either by H_2O or CO_2) are endothermic. In this study, a fairly large current density of 250 mA cm^{-2} was maintained during operation, which supplied sufficient O^{2-} for CH_4 oxidation and cause great heat dissipation. On the other hand, dry methane was directly pumped to the anode. It means that the amount of H_2O and CO_2 used for reforming reactions were determined by oxidation of CH_4. As a result, the overall reaction happened in the anode was exothermic rather than endothermic.

In Fig. 3d, the grain boundaries of the particles were clear and no carbon species were observed. It indicated that even if methane pyrolysis happened in the anode substrate, the reaction rate might be low and carbon species were so small that it is hard to be observed after 450 min.

Figure 5 shows the I–V characteristics of the tubular cell at different stages of cell operation. The open circuit voltage (OCV) of the cell was about 1.1 V, close to the theoretical value. This proved that the SOFC setup was gastight and the electrolyte film was sufficiently dense. After operating for 80 min ($t = 80$ min), the tubular SOFC reached a maximum power density of 350 mW cm^{-2} in CH_4. With the passage of some more time, some degradation of the cell performance was observed. No obvious concentration polarization was observed in all the I–V curves, even at a high current density of 800 mA cm^{-2}.

The electrochemical impedance spectra of the tubular SOFC at different stages of operation are shown in Fig. 6. All of the impedance spectra consisted of one semicircle. The high-frequency intercepts of the semicircles with the real axis, referred to ohmic resistance, almost coincided at a specific point, while the diameter of the semicircle, referred to polarization resistance (R_p), changed with time. After the fuel was switched from H_2 to CH_4 for 10 min ($t = 10$ min), R_p was only 0.7Ω cm^2. It increased to 1.42 and 1.55Ω cm^2 after 100 and 200 min, respectively. After some more time, it was found that R_p decreased a little with time. The variation of R_p might be caused by the partial pressure changes in the anode. The concentration of H_2 in the anode decreased and CH_4 increased with time. Due to the larger molecule and more stable characteristics of CH_4 [3, 19], the activation process is more difficult for CH_4 than for H_2. The porous microstructures of the anode substrate supplied sufficient pores for gas diffusion which made the concentration polarization small, whereas the activation polarization of the anode had little relationship with microstructure. In Fig. 5, no obvious concentration polarization was observed in the I–V curves, so the semicircle of the impedance spectra might be mainly caused by the activation process. The reason for the further decreasing of the polarization resistance with time remained unknown.

After the cell test, N_2 was fed to the anode till the cell was cooled down to room temperature. No carbon species were observed on the surface of the anode and the nickel felt in the anode room after operation. A small pin hole was found in the glass sealant at the bottom of tubular SOFC. It might be the reason for the degradation of the cell performance during operation.

Conclusions

A tubular SOFC with a double-layer anode has been prepared and operated with dry methane as fuel. A maximum power density of 350 mW cm^{-2} has been obtained for the tubular SOFC. The cell performance decreased and the operating temperature increased with time. After the cell was operated 450 min at a current density of 250 mA cm^{-2}, no carbon deposits were found on the surface of the double-layer anode. The cell performances under other current densities need to be examined in the future.

References

1. Park S, Vohs JM, Gorte RJ (2000) Nature 404:265
2. Mogensen M, Kammer K (2003) Annu Rev Mater Res 33:321
3. Koh J-H, Yoo Y-S, Park J-W, Lim HC (2002) Solid State Ionics 149:157
4. Baker UT, Metcalfe IS, Middleton PH, Steele BCH (1994) Solid State Ionics 72:328
5. Atkinson A, Barnett S, Gorte RJ, Irvine JTS, McEvoy AJ, Mogensen M, Singhal C, Vohs J (2004) Nat Mater 3:17
6. Sfeir J, Buffat PA, Möckli P, Xanthopoulos N, Vasquez R, Mathieu HJ, Van herle J, Thampi KR (2001) J Catal 202:229
7. Vernoux P, Gulllodo M, Fouletier J, Hammou A (2000) Solid State Ionics 135:425
8. Marina OA, Canfield NL, Stevenson JW (2002) Solid State Ionics 149:21
9. Park S, Craciun R, Vohs JM, Gorte RJ (1999) J Electrochem Soc 146:3603

10. Choudhary VR, Rane VH, Rajput AM (1997) Appl Catal A Gen 162:235
11. Eguchi K, Setoguchi T, Inoue T, Arai M (1992) Solid State Ionics 52:165
12. Uchida H, Suzuki H, Watanabe M (1998) J Electrochem Soc 145:615
13. Marina OA, Bagger C, Primdahl S, Mogensen M (1999) Solid State Ionics 123:199
14. Jiang Y, Virkar AV (2003) J Electrochem Soc 150:A942
15. Finnerty CM, Cunningham RH, Ormerod RM (2000) Radiat Eff Defect S 151:77
16. Ke K, Tsuchida S, Gunji A, Takahashi H, Ukai K, Mizutani Y, Sumi H, Yokoyama M, Waki K (2005) Electrochemical society proceedings 7:1317–1321
17. Jiang SP (2002) Solid State Ionics 146:1
18. Tu HY, Takeda Y, Imanishi N, Yamamoto O (1999) Solid State Ionics 117:277
19. Murray PE, Tsai T, Barnett SA (1999) Nat 400:649